

In Vitro Metabolism and Disposition of Honokiol in Rat and Human Livers

MICHAELA BÖHMDORFER,¹ ALEXANDRA MAIER-SALAMON,¹ BARBARA TAFERNER,² GOTTFRIED REZNICEK,³ THERESIA THALHAMMER,⁴ STEFFEN HERING,² ANTJE HÜFNER,⁵ WOLFGANG SCHÜHLY,⁶ WALTER JÄGER¹

¹Department of Clinical Pharmacy and Diagnostics, University of Vienna, A-1090 Vienna, Austria

²Department of Pharmacology and Toxicology, University of Vienna, A-1090 Vienna, Austria

³Department of Pharmacognosy, University of Vienna, A-1090 Vienna, Austria

⁴Institute of Pathophysiology, Medical University of Vienna, A-1090 Vienna, Austria

⁵Institute of Pharmaceutical Sciences, Department of Pharmaceutical Chemistry, Karl-Franzens-University Graz, A-8010 Graz, Austria

⁶Institute of Pharmaceutical Sciences, Department of Pharmacognosy, Karl-Franzens-University Graz, A-8010 Graz, Austria

Received 6 October 2010; revised 31 January 2011; accepted 14 February 2011

Published online 14 March 2011 in Wiley Online Library (wileyonlinelibrary.com). DOI 10.1002/jps.22536

ABSTRACT: The biotransformation of honokiol, a major constituent of the bark of *Magnolia officinalis*, was investigated in rat and human livers. When isolated, rat livers were perfused with 10 μ M honokiol and two metabolites, namely hydroxylated honokiol conjugated with glucuronic and sulfuric acid (M1) and honokiol monoglucuronide (M2), were quantified in bile and perfusate by high-performance liquid chromatography. The hepatic extraction ratio and clearance of honokiol was very high in rat liver (E : 0.99 ± 0.01 and 35.8 ± 0.04 mL/min, respectively) leading to very low bioavailability ($F = 0.007 \pm 0.001$). M2 formation was also highly efficient in human liver microsomes [$V_{\max}/K_m = 78.1 \pm 6.73$ μ L/(min mg)], which appeared to be catalyzed mainly by UDP-glucuronosyltransferases 1A1, A3, 1A8, and 1A10, indicating hepatic and extrahepatic glucuronidation. Monosulfation of honokiol to the minor metabolite honokiol monosulfate [$V_{\max}/K_m = 27.9 \pm 4.33$ μ L/(min mg)] by human liver cytosol was less pronounced and is mediated by sulfotransferases 1A1* 1, 1A1* 2, 1A2, 1A3, 1B1, and 1E1. P450-mediated oxidation of honokiol by liver microsomes, however, was below detection limit. In summary, this study established that glucuronidation and sulfation are the main metabolic pathways for honokiol in rat and human liver, suggesting their major contribution to clearance *in vivo*. © 2011 Wiley-Liss, Inc. and the American Pharmacists Association *J Pharm Sci* 100:3505–3516, 2011

Keywords: honokiol; hepatic metabolism; hepatic clearance; biliary excretion; glucuronidation; sulfation

INTRODUCTION

Honokiol (3',5-di-(2-propenyl)-1,1'-biphenyl-2,2'-diol) is a bioactive neolignan constituent of cortex magnoliae, derived from the Chinese medicinal plant *Magnolia officinalis*. The compound has several pharmacological properties; it is anti-inflammatory via inhibiting cyclooxygenase-2,^{1,2} antioxidative,³ antiplatelet,⁴ antiarrhythmic,⁵ antidepressant,⁶ and

anxiolytic.^{7,8} In addition, honokiol is a promising chemotherapeutic agent possessing antitumor activity without considerable toxicity. Recent studies show that honokiol inhibits angiogenesis *in vitro* and tumor growth *in vivo*,⁹ induces apoptosis in human colorectal carcinoma RKO cells,¹⁰ induces caspase-dependent apoptosis in B-cell chronic lymphocytic leukemia cells,¹¹ and inhibits *in vitro* and *in vivo* growth of breast cancer through induction of apoptosis and cell cycle arrest.¹²

Although much is known about the biological effects of honokiol, its metabolic pathway has not been identified. A study of the biotransformation of

Correspondence to: Walter Jäger (Telephone: +43-1-4277-55576; Fax: +43-1-4277-9555; E-mail: walter.jaeger@univie.ac.at)

Journal of Pharmaceutical Sciences, Vol. 100, 3506–3516 (2011)
© 2011 Wiley-Liss, Inc. and the American Pharmacists Association

its isomer magnolol (5,5'-diallyl-2,2'-biphenyldiol) demonstrated phase I and phase II metabolism. After magnolol was orally administered to rats, Hattori et al.¹³ showed the formation of tetrahydro-magnolol, 5-[(*E*)-1-propenyl]-5'-propyl-1,1'-biphenyl-2,2'-diol, 5-(2-propenyl)-5'-propyl-1,1'-biphenyl-2,2'-diol, isomagnolol, and 5-[(*E*)-1-propenyl]-5'-(2-propenyl)-1,1'-biphenyl-2,2'-diol in the urine and feces. An additional study by the same authors¹⁴ exhibited rapid absorption of magnolol from the gastrointestinal tract after oral administration of [ring-¹⁴C]-magnolol to rats. Blood radioactivity levels showed two peaks at 15 min and 8 h, suggesting enterohepatic circulation of magnolol and its metabolites. Radioactivity was distributed to a variety of organs with [ring-¹⁴C]-magnolol-2-O-glucuronide being the major metabolite in the bile and blood.

In this study, we investigated the metabolism of honokiol in rat and human livers by using liver microsomes, liver cytosol, and isolated perfused rat liver. Furthermore, we identified the chemical structure of honokiol metabolites by liquid chromatography–mass spectrometry (LC/MS) and the isoenzymes responsible for their formation.

MATERIALS AND METHODS

Materials

Honokiol (purity >98%) was obtained by demethylation (via Grignard reaction) of 4'-*O*-methylhonokiol.¹⁵ Uridine 5'-diphosphoglucuronic acid (UDPGA; 98%–100% purity), dimethyl sulfoxide (DMSO), 3'-phosphoadenosine-5'-phosphosulfate (PAPS; 78% purity), dithiothreitol (DTT), and the constituents for the nicotinamide adenine dinucleotide phosphate (NADPH)-generating system were obtained from Sigma (Munich, Germany). Methanol and water were of high-performance liquid chromatography (HPLC) grade (Merck, Darmstadt, Germany). Human liver microsomes (protein content 20 mg/mL) from one male and two females (mean age 63 years, range 45–78 years), human liver cytosol (protein content 20 mg/mL) from one male and two females (mean age 65 years, range 53–78 years), baculovirus-infected insect cells containing the cDNA for human UDP-glucuronosyltransferases (UGTs) 1A1, 1A3, 1A4, 1A6, 1A7, 1A8, 1A9, 1A10, 2B4, 2B7, 2B15, and 2B17 were obtained from BD Biosciences (Woburn, Massachusetts). Human sulfotransferases (SULTs) 1A1* 1, 1A1* 2, 1A2, 1A3, 1B1, 1E1, and 2A1 expressed in *Escherichia coli* were purchased from Cypex (Dundee, UK). The catalytic activities of human liver microsomes, human liver cytosol, recombinant UGTs, and recombinant SULTs were as described in the data sheets provided by the manufacturers. All other

chemicals and solvents were of analytical grade and were used without further purification.

Liver Perfusion

The study was approved by the Animal Experimentation Ethics Committee of the Austrian Ministry for Education, Science and Culture. Male Wistar rats (body weight = 275 ± 43.5 g; liver weight = 11.8 ± 2.1 g) were purchased from the Department of Animal Research and Genetics of the Medical University of Vienna, Austria. Animals were housed in a temperature- and humidity-controlled room under a 12-h light–dark cycle with free access to water and food. Single-pass liver perfusion experiments were carried out using the techniques previously described.¹⁶ The total volume of the perfusion reservoir was 2500 mL. Perfusions were conducted using a freshly prepared Krebs–Henseleit buffer (KHB) at pH 7.4, equilibrated with 95% O₂/5% CO₂ during the whole procedure at a constant flow rate of 36 mL/min. The temperature of the perfusion cabinet and perfusion medium was thermostatically controlled at 37°C, and the perfusion pressure was constantly monitored. After 30 min of perfusion with KHB, stock solutions of honokiol (10 mM in DMSO) were added to give a final concentration of 10 μM. To test the stability of honokiol under perfusion conditions, this solution was applied in a control experiment to a perfusion model without a liver. The viability of the liver was assessed by its visual appearance and by checking the perfusate flow. At the end of the experiment, the liver was dried, weighed, and frozen (–80°C) until analysis.

Tissue Analysis

Liver tissue was thawed on ice at 4°C, weighed into glass test-tubes (approx. 500 mg), mixed with a five-fold amount of 50 mM potassium phosphate buffer (pH 7.4), and then minced using an Ultra-Turrax® homogenizer (IKA, Staufen, Germany) four times for 10 s each on ice. Two milliliters of homogenates were first centrifuged at 13,000 × *g* for 10 min, and proteins were eliminated by a second centrifugation by adding methanol (500 μL) to 250 μL of the supernatant. Eighty microliters of the remaining supernatant was injected onto the HPLC column.

Determination of Honokiol and Its Metabolites in Bile, Perfusate, and Liver Tissue

To study time-dependent first-pass metabolism, bile (30–50 μL) and perfusate (approx. 1.5 mL) were collected every 5 min for 90 min, immediately frozen on dry ice, and stored at –80°C. Prior to analysis, bile and perfusate samples were centrifuged (5000 × *g* for 5 min). Eighty microliters of diluted bile samples (5 μL supernatant + 95 μL distilled water) and 80 μL of perfusate supernatant were injected

onto the HPLC column. The determination of honokiol and its metabolites was performed using an UltiMate 3000 HPLC system (Dionex, Sunnyvale, California) equipped with a Hypersil BDS-C₁₈ column (5 μ m, 250 \times 4.6 mm ID; Thermo Fisher Scientific, Inc., Waltham, Massachusetts), preceded by a Hypersil BDS-C₁₈ precolumn (5 μ m, 10 \times 4.6 mm ID), at a flow rate of 1 mL/min and a column temperature of 15°C. The mobile phase consisted of a continuous linear gradient mixed from 5 mM ammonium acetate/acetic acid buffer, pH 7.4 (mobile phase A), and methanol (mobile phase B); honokiol and its metabolites eluted according to their lipophilicity. The mobile phase was filtered through a 0.45- μ M filter (HVLPO4700; Millipore, Vienna, Austria). The gradient ranged from 20% B at 0 min to 40% B at 10 min, and linearly increased to 90% B at 22 min, at which it remained constant for 5 min. The percentage of methanol was decreased within 1 min to 20%, in order to equilibrate the column for 7 min before application of the next sample. Quantification of honokiol and its metabolites were monitored at 294 nm. Calibration of the chromatogram was accomplished using the external standard method. As standards of the metabolites were not available, quantification of metabolites was based on the assumption that the unknown metabolites had molar extinction coefficients similar to that of honokiol. Linear calibration curves were obtained from the peak areas of honokiol and its metabolites to the external standard honokiol by spiking drug-free bile with standard solutions of honokiol to give a concentration range of 0.1–100 μ g/mL (average correlation coefficients were >0.99).

Phase I Metabolism of Honokiol by Human Liver Microsomes

Microsomes (1 mg/mL), NADPH (1 mM), isocitric acid (5 mM), and isocitric dehydrogenase (0.5 U/mL) were preincubated for 5 min at 37°C in 0.05 M phosphate buffer, pH 7.4 (final volume 1.0 mL). The reaction was started by the addition of honokiol in DMSO (40 and 80 μ M) and its metabolism was assessed by HPLC after 30-min incubation at 37°C.

Effect of Detergents on Honokiol Glucuronidation

UDP-glucuronosyltransferases proteins are located in the endoplasmic reticulum and are sometimes enzymatically latent. Detergents can be used in order to obtain the maximal activity by disrupting the integrity of the membranes.¹⁷ We examined the effect of low solubilizing concentrations of some common detergents on the catalytic activity of UGTs involved in honokiol glucuronidation. Human liver microsomes (final concentration 0.5 mg proteins per milliliter) were preincubated on ice for 30 min with 25, 50, or 100 μ g detergent per milligram microsomal protein; the detergent used was Triton X-100, Brij

35, Brij 58, alamethicin, or digitonin. Then, magnesium chloride (10 mM), D-saccharic acid-1,4-lactone (5 mM), and honokiol (final concentration 40 μ M) in DMSO were added to 50 mM potassium phosphate buffer (pH 7.4) in a total volume of 100 μ L. The glucuronidation assay was initiated by adding 3 mM UDPGA, and the metabolism of honokiol was assessed after 20-min incubation at 37°C as described above. Control experiments in the absence of detergent were run in parallel.

Glucuronidation of Honokiol by Human Liver Microsomes and Recombinant UGT Isoenzymes

Human liver microsomes (50 μ g of protein) and microsomes prepared from baculovirus-infected insect cells (BTI-TN-5B1–4; 25 μ g of protein) containing the cDNA for human UGTs 1A1, 1A3, 1A4, 1A6, 1A7, 1A8, 1A9, 1A10, 2B4, 2B7, 2B15, and 2B17, respectively, were preincubated with alamethicin (25 μ g/mg protein) on ice for 30 min. Next, magnesium chloride (10 mM), D-saccharic acid-1,4-lactone (5 mM), and honokiol (final concentrations 10–400 μ M) in DMSO were added to 50 mM potassium phosphate buffer (pH 7.4) in a total volume of 100 μ L. Reactions were initiated by the addition of 3 mM UDPGA, and the samples were incubated for 20 min at 37°C. After the reactions were terminated by the addition of 200 μ L methanol, the samples were centrifuged (13000 $\times g$ for 5 min). A total of 80 μ L of the supernatant was injected onto the HPLC column and analyzed under conditions identical to those mentioned above. Glucuronidation of honokiol was not observed when using insect cells infected with wild-type baculovirus (*Autographa californica*) and in the absence of UDPGA. Enzyme kinetics for glucuronidation of honokiol by recombinant UGTs was further evaluated by incubation of UGTs 1A1, 1A3, 1A8, and 1A10 (with honokiol (10–400 μ M) under conditions identical to those mentioned above.

Sulfation of Honokiol by Human Liver Cytosol and Recombinant Sult Isoenzymes

Human liver cytosol (50 μ g of protein) and cytosolic extracts prepared from *E. coli* (containing cDNA for human SULTs 1A1* 1, 1A1* 2, 1A2, 1A3, 1B1, 1E1, and 2A1; 25 μ g of protein) were incubated in a reaction mixture containing 1–400 μ M of honokiol (final concentration), 50 μ M PAPS, 7.4 mg/mL DTT, 0.05 M potassium phosphate (pH 7.4), 150 mM KCl, 50 mM Tris (pH 7.5), and 2 mM ethylenediaminetetraacetic acid in a total volume of 100 μ L. PAPS and DTT stock solutions were prepared fresh each day. Reactions were initiated by adding PAPS, and the samples were incubated for 20 min at 37°C. After the reactions had been terminated by the addition of 200 μ L methanol, the samples were centrifuged (13000 $\times g$ for 5 min) and 80 μ L of the supernatant was injected

onto the HPLC column. Sulfation of honokiol was not observed in the absence of PAPS and when using control cytosol from *E. coli* containing the vector only. Enzyme kinetics for honokiol sulfation by SULTs 1A1* 1, 1A1* 2, 1A2, 1A3, 1B1, and 1E1 were evaluated by incubation of the recombinant enzymes with honokiol (1–400 μ M) under identical conditions as those mentioned above.

Identification of Honokiol Metabolites

Liquid chromatography–mass spectrometry analyses of diluted bile samples (5 + 95 μ L water), human liver microsomes, and human liver cytosol (40 + 60 μ L methanol) were performed on an Ultimate 3000 RSLC-series system (Dionex, Germering, Germany) coupled to a mass spectrometer equipped with an orthogonal electrospray ionization source. Negative ion polarity was used to acquire mass spectra from m/z equals to 150–900 amu in scanning mode. Metabolites hydroxylated honokiol conjugated with glucuronic and sulfuric acid (M1) and honokiol monoglucuronide (M2) were analyzed on an AB Sciex API 4000 triple quadrupole mass spectrometer using the following parameters: -4.1kV capillary voltage, 20 psi nebulizer (N_2), 10 L/min dry gas flow (N_2), and 340°C dry temperature, and scan m/z 100–1000/s. Metabolite honokiol monosulfate (M3) was identified by a 3D quadrupole ion trap mass spectrometer (HCT; Bruker Daltonics, Bremen, Germany) with the following settings: 3.7 kV capillary voltage, 22 psi nebulizer (N_2), 8 L/min dry gas flow (N_2), and 340°C dry temperature. The HPLC column, injection volume, mobile phase, gradient, and flow rate were identical to those used for the analytical HPLC assay (see above).

Data Analysis

Pharmacokinetic parameters of the liver perfusion were calculated using data recorded after steady-state conditions were reached. Inflow and outflow molar concentrations and biliary excretion were averaged before inclusion into the pharmacokinetic equations given below.

The availability (F) of honokiol was calculated using the following equation:

$$F = \frac{X_{\text{out}}}{X_{\text{in}}} \quad (1)$$

where X_{in} is the administered dose (amount of honokiol applied to the liver during 90 min) and X_{out} is the amount of honokiol excreted in the effluent perfusate over 90 min.

The hepatic clearance (Cl) of honokiol was calculated as follows:

$$\text{Cl} = E \times \text{perfusate flow rate} \quad (2)$$

where E is the extraction rate ($1-F$).

The amount of honokiol and its metabolites excreted into bile during 90 min of perfusion, expressed as a percentage of the administered dose (f_{bile}), was calculated as:

$$f_{\text{bile}} = \frac{X_{\text{C}} \times \text{bile flow} \times \text{liver weight} \times 100}{X_{\text{in}}} \quad (3)$$

where X_{in} is the amount of honokiol applied to the liver during 90 min by single-pass perfusion and X_{C} is the cumulative amount of honokiol and the metabolites M1 and M2 in bile.

The amount of honokiol and its metabolites excreted into perfusate during 90 min of perfusion, expressed as a percentage of the administered dose ($f_{\text{perfusate}}$), was then calculated as:

$$f_{\text{perfusate}} = \frac{X_{\text{C}} \times 100}{X_{\text{in}}} \quad (4)$$

where X_{in} is the amount of honokiol applied to the liver during 90 min by single-pass perfusion and X_{C} is the cumulative amount of honokiol and the metabolites M1 and M2 in perfusate.

Metabolic clearance of honokiol via its metabolites M1 and M2 (Cl_{Met}) was calculated as:

$$\text{Cl}_{\text{Met}} = \frac{X_{\text{bile}} + X_{\text{perfusate}}}{X_{\text{in}}} \times \text{perfusate flow rate} \quad (5)$$

where X_{in} is the amount of honokiol applied to the liver during 90 min by single-pass perfusion, X_{bile} is the cumulative concentration of the metabolites M1 and M2 in bile, and $X_{\text{perfusate}}$ is the cumulative concentration of the metabolites M1 and M2 in perfusate. Unless otherwise indicated, values are expressed as mean value \pm SD averaged from three individual experiments.

In the various glucuronidation and sulfation assays, each incubation step was performed at least in triplicate, and the results were expressed as mean \pm SD. Formation rates calculated for the recombinant enzymes were mathematically adjusted to the individual catalyzing activities of liver microsomal and liver cytosolic samples as given by the company. The data were fitted to Michaelis–Menten (hyperbolic) and substrate inhibition models. The coefficient of determination (R^2) was used to determine the quality of a fit to a specific model. Kinetic parameters were estimated using Prism (version 5.0; GraphPad Software Inc., San Diego, California) with Michaelis–Menten (Eq. 6) and substrate inhibition kinetics (Eq. 7).

$$V = V_{\text{max}} \times \frac{S}{(K_{\text{m}} + S)} \quad (6)$$

$$V = \frac{V_{\max}}{\left(1 + \frac{K_m}{S} + \frac{S}{K_i}\right)} \quad (7)$$

where V is the rate of reaction, V_{\max} is the maximum velocity, K_m is the Michaelis constant, S is the substrate concentration, and K_i is the inhibition constant. The enzymatic efficacy, which is defined as the V_{\max}/K_m ratio, quantifies the glucuronidation capacity and corresponds to the intrinsic clearance.

RESULTS

Metabolism and Disposition of Honokiol in Perfused Rat Livers

After perfusion of isolated livers of male Wistar rats with $10 \mu\text{M}$ honokiol for 90 min, native honokiol (retention time $T_R = 26.9$ min) as well as the two metabolites M1 ($T_R = 16.8$ min) and M2 ($T_R = 21.9$ min) could be detected in bile and perfusate (Fig. 1a). The kinetics of the excretion of honokiol and its metabolites after application of honokiol are demonstrated in Figures 2a–2c. Biliary secretion of unconjugated honokiol reached an early steady state after 10 min, with an average excretion rate of 8.23 ± 1.03 pmol/g liver per minute. However, excretion of the metabolites M1 and M2 showed a maximum after 45 min (mean values = 369 ± 107 and 798 ± 179 pmol/g liver per minute, respectively) followed by a distinct decrease until the end of perfusion (mean values after 90 min = 180 ± 40.5 and 493 ± 178 pmol/g liver per minute, respectively). In contrast to the rapid steady state seen in the bile, efflux of the parent drug into perfusate reached a plateau only after 40 min (maximum value = 217 ± 116 pmol/g liver per minute). Efflux of M1 and M2 continuously increased during 90 min of perfusion to 314 ± 87 and 1496 ± 690 pmol/g liver per minute, respectively.

The cumulative biliary excretion of honokiol, M1, and M2 was moderate, representing only 0.03 ± 0.01 , 0.87 ± 0.38 , and $2.03 \pm 0.36\%$ (0.66 ± 0.13 , 21.1 ± 5.86 , and 52.8 ± 15.7 nmol/g in liver per 90 min, respectively), respectively, of the administered dose of $10 \mu\text{M}$ (see Table 1; Fig. 3). The total amounts of M1 and M2 excreted into effluent perfusate over 90 min were 4.5- and 1.5-fold lower compared with their biliary excretion (4.53 ± 3.47 , 34.4 ± 21.1 nmol/g in liver per 90 min, respectively) indicating preferential excretion of metabolites into bile. The total efflux of honokiol, however, was 25-fold higher than in bile (16.5 ± 0.91 nmol/g in liver per 90 min). Remarkably, the total amount of native honokiol but not of M1 and M2 in the liver tissue of Wistar rats over 90 min of perfusion was high, amounting up to $80.0 \pm 5.5\%$ of the applied dose. Only $1.8 \pm 0.29\%$ and $10.4 \pm 4.5\%$ of M1 and M2 were found in liver tissue, respectively (Fig. 3).

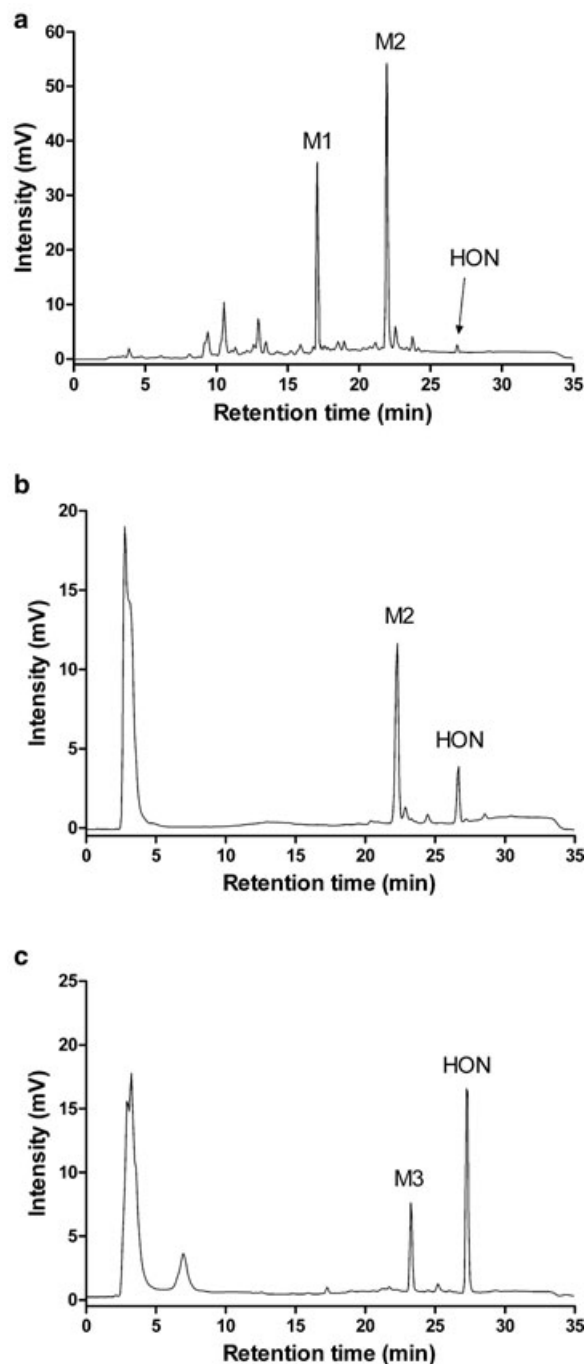


Figure 1. Representative HPLC chromatograms of honokiol (HON) and its metabolites M1, M2, and M3 (a) in bile from Wistar rats after 60 min of perfusion with $10 \mu\text{M}$ honokiol, (b) in human liver microsomes after incubation with $40 \mu\text{M}$ honokiol in the presence of uridine 5'-diphosphoglucuronic acid, and (c) in human liver cytosol after incubation with $40 \mu\text{M}$ honokiol in the presence of 3'-phosphoadenosine-5'-phosphosulfate.

Pharmacokinetic parameters describing the disposition of honokiol in the liver of Wistar rats were determined by standard techniques (Eqs. 1 and 2) using data from effluent perfusate samples collected

Table 1. Disposition of Honokiol and Its Metabolites M1 and M2 in the Isolated Perfused Wistar Rat Liver

	Cl (mL/min)	<i>F</i>	<i>E</i>	<i>f</i> _{bile} (%)	<i>f</i> _{perfusate} (%)	<i>f</i> _{liver} (%)	Cl _{Met} (mL/min)
M1	—	—	—	0.87 ± 0.38	0.17 ± 0.11	1.80 ± 0.29	0.31 ± 0.12
M2	—	—	—	2.03 ± 0.36	1.26 ± 0.48	10.4 ± 4.51	0.92 ± 0.26
Honokiol	35.8 ± 0.04	0.007 ± 0.001	0.99 ± 0.01	0.03 ± 0.01	0.66 ± 0.11	80.0 ± 5.53	—

Perfusions were performed with 10 μM honokiol for 90 min using a single pass model.

Cl, hepatic clearance of honokiol; *F*, bioavailability of honokiol; *E*, hepatic extraction rate of honokiol; Cl_{Met}, metabolic clearance.

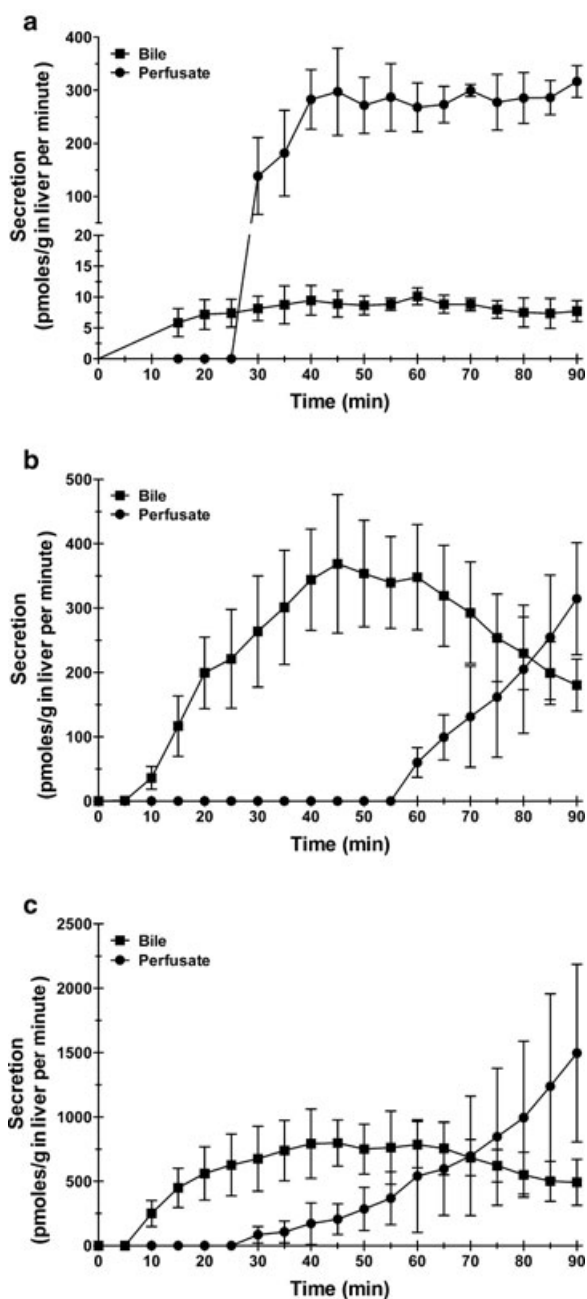


Figure 2. Time course of biliary excretion and efflux into perfusate of (a) honokiol and its metabolites (b) M1 and (c) M2 in Wistar rats when 10 μM honokiol was applied to the liver. Data are expressed as pmol/g liver per minute ± SD (*n* = 3).

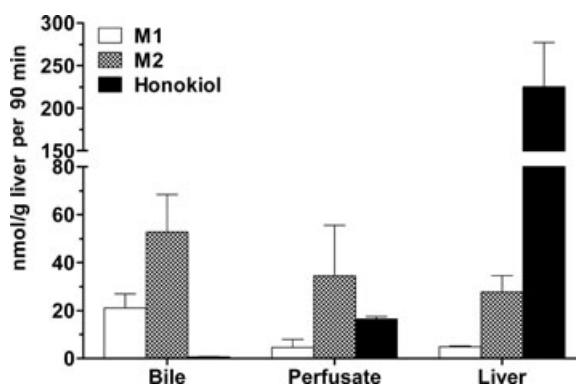


Figure 3. Disposition of honokiol and its metabolites M1 and M2 in Wistar rats after 90 min perfusion with 10 μM honokiol. Data are expressed as nmol/g liver per 90 min ± SD (*n* = 3).

over 90 min after addition of honokiol. On the basis of the extensive accumulation in liver tissue, honokiol has an extremely low bioavailability (*F*: 0.007 ± 0.001); more than 99% of the parent drug is extracted from the liver within the first liver passage (Table 1). Thus, the almost quantitative extraction results in a high clearance rate of 35.8 ± 0.04 mL/min, which approached the average perfusate flow rates. A proposed metabolic pathway of honokiol in the liver of Wistar rats is shown in Figure 6.

Metabolism of Honokiol in Human Livers

Metabolism of honokiol was further assessed in human livers. In contrast to rat liver, NADPH-dependent formation of phase I biotransformation products was below detection limit in human liver microsomes. However, when human liver microsomes and cytosol were incubated with honokiol in the presence of UDPGA and PAPS, respectively, two metabolites, namely M2 and M3 could be identified (Figs. 1b and 1c). ReSULTs from preliminary studies to optimize the incubation conditions for honokiol glucuronidation and sulfation showed that formation of M2 and M3 was linear with time up to 60 min at microsomal protein concentrations of 0.25–2 mg/mL. As shown in Figure 4, both glucuronidation and sulfation of honokiol by human livers exhibited substrate inhibition with comparable *K_i* values of 163 ± 22.6 and

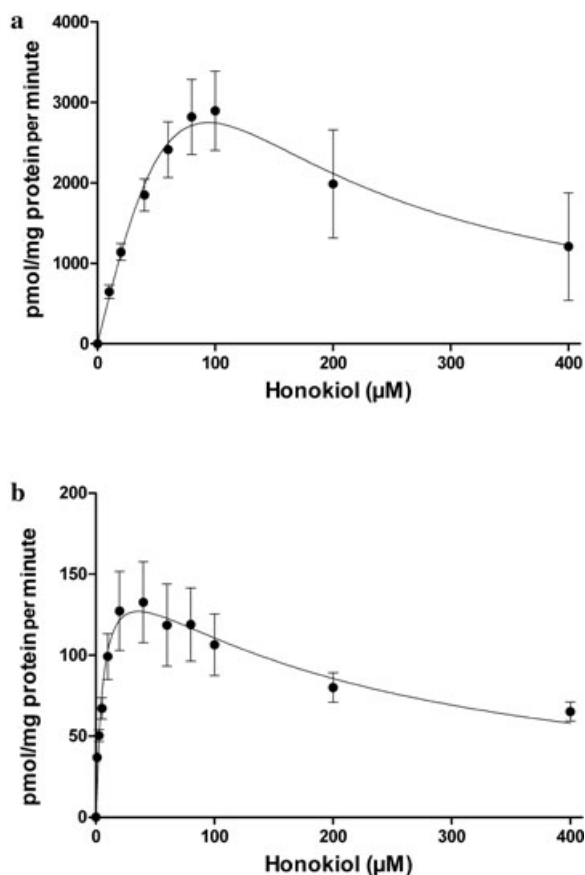


Figure 4. Kinetics of formation of (a) M2 in human liver microsomes and (b) M3 in human liver cytosol normalized to protein content as a function of honokiol concentration. Liver microsomes and cytosol were incubated with honokiol for 20 min at 37°C in the presence of uridine 5'-diphosphoglucuronic acid and 3'-phosphoadenosine-5'-phosphosulfate, respectively. Data are expressed as mean \pm SD ($n = 3$).

$207 \pm 88.2 \mu\text{M}$, respectively. The K_m value for honokiol glucuronidation, however, was 14-fold higher than that for sulfation (85.5 ± 10.2 vs. $6.14 \pm 2.32 \mu\text{M}$) indicating a preferable sulfate conjugation at lower substrate concentrations (see Tables 2 and 3). Figure 6 shows the proposed biotransformation pathway of honokiol in human liver.

Glucuronidation of Honokiol by Recombinant UGTs

Twelve recombinant human UGTs of family 1 and 2 were incubated with honokiol ($40 \mu\text{M}$) for 20 min after pretreatment with the solubilizing agent alamethicin. This initial screening showed that UGTs 1A1, 1A3, 1A6, 1A7, 1A8, 1A9, 1A10, 2B7, 2B15, and 2B17 glucuronidated honokiol to a single metabolite to varying extents (Fig. 5a). Among these isoforms, the formation of the metabolite was preferentially catalyzed by UGTs 1A10 [35.8%; $3293 \pm 2.55 \text{ pmol}/(\text{mg min})$] and 1A3 [28.2%; $2601 \pm 16.3 \text{ pmol}/(\text{mg min})$], but reached 9.8% [$901 \pm 7.50 \text{ pmol}/(\text{mg min})$] and 9.3% [$858 \pm$

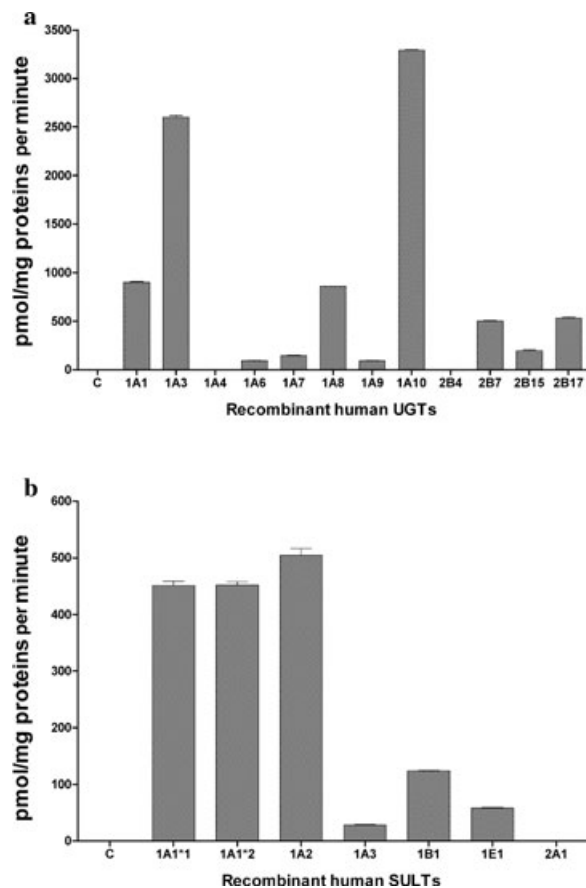


Figure 5. Rate of (a) M2 formation in recombinant human UDP-glucuronosyltransferases (UGTs) and (b) M3 formation in recombinant human sulfotransferases (SULTs) normalized to protein content as a function of honokiol concentration. Recombinant human UGTs and SULTs were incubated with $40 \mu\text{M}$ honokiol for 20 min at 37°C in the presence of uridine 5'-diphosphoglucuronic and 3'-phosphoadenosine-5'-phosphosulfate, respectively. Data are shown as mean \pm SD ($n = 3$).

$1.01 \text{ pmol}/(\text{mg min})$] with UGTs 1A1 and 1A8, respectively. Only a minor amount ($\sim 5\%$) of the metabolite was formed with UGTs 2B17 and 2B7. UGTs 1A6 and 1A9 exhibited low catalytic activity for the formation of M2, each contributed to less than and equal to 1% glucuronidation of the substrate. No detectable formation of M2 was seen with UGTs 1A4 and 2B4.

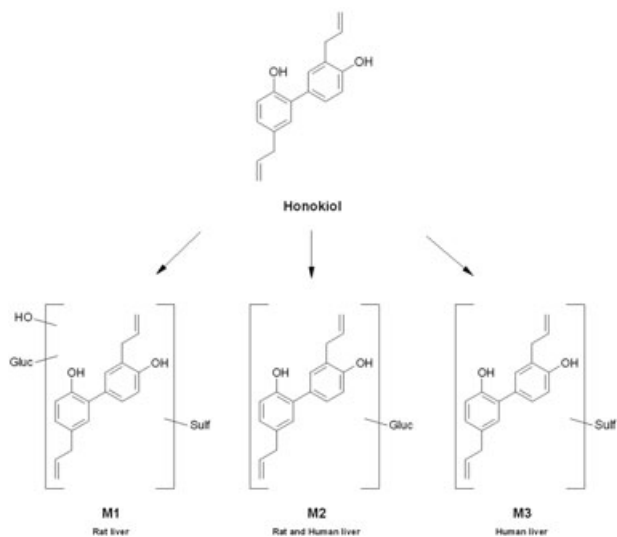
A comparative kinetic analysis was performed using honokiol concentrations ranging from 1 to $400 \mu\text{M}$ to investigate the catalytic activities of UGT1A1, UGT1A3, UGT1A8, and UGT1A10 for honokiol glucuronidation. The apparent enzyme kinetic parameters for M2 of the recombinant isoenzymes UGT1A1, UGT1A8, and UGT1A10 were estimated by fitting to the substrate inhibition model (Eq. 7), whereas the formation of the honokiol glucuronide in UGT1A3 followed classical Michaelis–Menten kinetics (Eq. 6). Data on kinetics are reported in Table 2. Interestingly, the formation of honokiol glucuronide resulted in

Table 2. Kinetic Parameters of M2 Formation by Human Liver Microsomes and Recombinant Human UGT1A1, UGT1A3, UGT1A8, and UGT1A10

	Model	K_m (μM)	V_{\max} (pmol/(mg min))	V_{\max}/K_m ($\mu\text{L}/(\text{min mg})$)	K_i (μM)
Liver microsomes	Substrate inhibition	85.5 ± 10.2	6677 ± 525	78.1 ± 6.73	163 ± 22.6
1A1	Substrate inhibition	1.82 ± 0.43	932 ± 19.9	512 ± 43.1	1246 ± 202
1A3	Michaelis–Menten	3.67 ± 0.62	3046 ± 52.5	830 ± 16.7	NA
1A8	Substrate inhibition	0.84 ± 0.46	747 ± 18.3	893 ± 27.2	1709 ± 411
1A10	Substrate inhibition	1.32 ± 0.17	3592 ± 31.4	2729 ± 103	1392 ± 101

Data are shown as mean \pm SD of three determinations.
NA, not applicable.

similar V_{\max} values for UGT1A3 and UGT1A10 (3046 and 3592 pmol/mg proteins per minute, respectively), but showed a 2.8-fold higher K_m value for UGT1A3 compared with UGT1A10. In addition, the intrinsic clearance estimates (V_{\max}/K_m) revealed 3.1- to 5.3-fold higher values for UGT1A10 compared with those for UGT isoenzymes 1A1, 1A3, and 1A8. The K_i estimates for UGTs 1A1, 1A10, and 1A8 were all high, with values of 1246, 1392, and 1709 μM , respectively, indicating only minor substrate inhibition.


Figure 6. Proposed metabolic pathway of honokiol in rat and human liver.

Sulfation of Honokiol by Recombinant SULTs

The screening of seven recombinant human SULTs of family 1 and 2 for honokiol sulfation activity revealed that SULTs 1A1*1, 1A1*2, 1A2, 1A3, 1B1, and 1E1 are able to catalyze the sulfation of honokiol to the monosulfate M3, however, to varying extents (Fig. 5b). At 40 μM , honokiol sulfation was almost equally catalyzed by SULT1A1*1 [27.8%; 450 \pm 7.88 pmol/(mg min)], SULT1A1*2 [27.9%; 452 \pm 6.13 pmol/(mg min)], and SULT1A2 [31.2%; 504 \pm 11.8 pmol/(mg min)] but reached 7.65% [123 \pm 0.89 pmol/(mg min)] with SULT1B1. The isoforms SULT1A3 and SULT1E1 exhibited only low catalytic activities for M3 formation ($\leq 4\%$). No formation of M3 was seen with SULT2A1. A similar sulfation pattern by all SULT isoforms was also seen at 5 μM honokiol (data not shown).

A comparative kinetic analysis was performed using honokiol concentrations ranging from 1 to 400 μM to investigate the catalytic activities of SULTs 1A1*1, 1A1*2, 1A2, 1A3, 1B1, and 1E1 for honokiol sulfation (kinetic parameters are reported in Table 3). M3 formation in SULTs 1A1*1, 1A1*2, 1A2, and 1E1 exhibited distinct substrate inhibition (Eq. 7) with K_i values ranging from 24.8 \pm 11.3 to 262 \pm 59.8 μM . In contrast, formation of M3 by SULTs 1A3 and 1B1 displayed Michaelis–Menten kinetics. K_m and V_{\max} values for SULTs 1A3, 1B1, and 1E1 were much lower compared with SULTs 1A1*1, 1A1*2, and 1A2. Intrinsic clearance values (V_{\max}/K_m) quantifying the sulfation capacity of the enzyme source,

Table 3. Kinetic Parameters of M3 Formation by Human Liver Cytosol and Recombinant Human SULT1A1*1, SULT1A1*2, SULT1A2, SULT1A3, SULT1B1, and SULT1E1

	Model	K_m (μM)	V_{\max} (pmol/(mg min))	V_{\max}/K_m ($\mu\text{L}/(\text{min mg})$)	K_i (μM)
Liver Cytosol	Substrate inhibition	6.14 ± 2.32	171 ± 24.4	27.9 ± 4.33	207 ± 88.2
1A1*1	Substrate inhibition	48.0 ± 17.4	1270 ± 295	26.5 ± 9.71	32.6 ± 10.7
1A1*2	Substrate inhibition	42.1 ± 25.2	1509 ± 520	35.9 ± 13.8	24.8 ± 11.3
1A2	Substrate inhibition	92.3 ± 39.4	1668 ± 504	18.1 ± 5.78	79.8 ± 20.4
1A3	Michaelis–Menten	1.07 ± 0.36	23.5 ± 5.72	22.0 ± 6.91	NA
1B1	Michaelis–Menten	0.41 ± 0.19	117 ± 32.1	285 ± 86.7	NA
1E1	Substrate inhibition	0.85 ± 0.32	59.5 ± 17.4	69.9 ± 21.9	262 ± 59.8

Data are shown as mean \pm SD of three determinations.
NA, not applicable.

however, were as follows: 1B1 > 1E1 > 1A1* 2 > 1A1* 1 > 1A3 > 1A2.

Identification of Honokiol Metabolites

Structural identification of M1–M3 was conducted by LC/MS. Negative ion mass spectra of bile samples, human liver microsomes, and human liver cytosol revealed stable molecular ions at m/z 265, 537, 441, and 345 amu., in agreement with the molecular weights of native honokiol, M1 (honokiol + 16 amu + 80 amu + 176 amu), M2 (honokiol + 176 amu), and M3 (honokiol + 80 amu). Because of insufficient amounts of these metabolites in bile and human liver microsomes and cytosol and a lack of commercially available standards, it was not possible to determine the exact structure of honokiol metabolites by nuclear magnetic resonance (NMR).

DISCUSSION

Honokiol is one of the main components of *M. officinalis* bark,¹⁸ which has been extensively used as a traditional medicine in China and Japan. Recent studies demonstrated that honokiol exhibits various pharmacological properties without considerable toxicity.

In the present study, hepatic biotransformation and disposition of honokiol and its metabolites were investigated for the first time by perfusing isolated male Wistar rat livers with 10 μ M of honokiol. This concentration was chosen based on daily intakes of 250–750 mg of an extract standardized for the primary active ingredients (typically 1%–2% honokiol and magnolol). During 90 min the perfused liver extracted more than 99% of applied honokiol; steady-state concentrations were achieved within 30 min after commencement of infusion. However, only 0.03% of the administered dose was found in bile and 0.66% in the effluent perfusate. This is in accordance with a previous study in rats, also demonstrating very low plasma levels of unconjugated honokiol ($C_{\max} < 90$ ng/mL) after rectal administration of 13.5 mg/kg honokiol,¹⁹ indicating low bioavailability based on extensive biotransformation. The high hepatic clearance of honokiol (35.8 ± 0.04 mL/min) may also be explained by its marked tendency to accumulate in liver tissue (80.0% of the applied dose).

On the contrary, hepatic biotransformation of honokiol was high, amounting to 16.5% of the applied dose; 22.4% of total metabolites were retained in the liver tissue, 50.6% were excreted into bile, and 27% were excreted into effluent perfusate. LC/MS analysis of bile and perfusate revealed the formation of two metabolites, namely a glucuronidated and sulfated

monohydroxyhonokiol (M1) and a monoglucuronide (M2). Low recovery of these compounds did not allow further structural identification by NMR. Interestingly, glucuronidation of honokiol leading to M2 formation was clearly favored in the rat liver, amounting up to 13.5% of the applied dose, whereas M1 formation seemed to be a minor metabolic pathway (3% of the administered drug).

Extensive glucuronidation is in accordance with studies of Hattori et al.,¹⁴ who showed pronounced glucuronidation and high accumulation of the structural isomer magnolol in rat liver. Pharmacokinetic studies also revealed very similar half-lives of honokiol and magnolol in rat plasma (49.22 ± 6.68 and 56.24 ± 7.30 min vs. 49.05 ± 5.96 and 49.58 ± 6.81 min) after intravenous administration of 5 and 10 mg/kg, respectively, indicating similar biotransformation and disposition.^{20,21}

Analogous to rat liver, phase II metabolism was also predominant in human liver with about threefold higher intrinsic clearance values for monoglucuronide (M2) formation than for monosulfation (M3). Metabolite formation, however, was dose dependent as sulfation clearly prevailed in the lower honokiol concentrations (1–40 μ M). When the initial honokiol concentration further increased, total sulfate formation in human liver cytosol dropped dramatically (200 μ M honokiol) based on noncompetitive substrate inhibition. This is in accordance with recent data from our laboratory, in which we demonstrated that in human liver cytosol and in human intestinal Caco-2 cells, sulfation of the natural polyphenolic compound resveratrol was also best characterized by the substrate inhibition model.^{22,23}

In contrast to rat liver, cytochrome P450-dependent hydroxylation was below detection limit in human liver indicating species-related differences in honokiol metabolism.

Using recombinant UGT isoenzymes, we further demonstrated that honokiol is mainly glucuronidated by UGTs 1A1, 1A3, 1A8, and 1A10. The kinetic profiles of M2 formation by UGTs 1A1, 1A8, and 1A10 were similar, but that of UGT1A3 was markedly different. M2 formation by UGT1A3 was consistent with classical Michaelis–Menten kinetics, with a 2.0- to 4.4-fold higher K_m value compared with the isoforms UGTs 1A1, 1A8, and 1A10, which displayed substrate inhibition kinetics.

Our data also demonstrated hepatic as well as extrahepatic glucuronidation of honokiol. UGTs 1A1 and 1A3 have been observed in the liver and small intestine. UGTs 1A8 and 1A10 are not expressed in the liver but are expressed in the small intestine and colon.^{24,25} All of these UGTs will therefore contribute to the honokiol glucuronidation in human and rat intestines.

Analogously, human recombinant SULT isoforms were screened for honokiol sulfation. We found that several of these isoenzymes are responsible for the conjugation of honokiol with sulfuronic acid. Although SULTs 1A1* 1, 1A1* 2, and 1A2 demonstrated far higher sulfation rates *in vitro* at 5 and 40 μM , *in vivo* only SULTs 1A3, 1B1, and 1E1 may contribute significantly to honokiol sulfation based on very low K_m values (0.41–1.07 μM).

As demonstrated for glucuronidation, we could also show hepatic as well as extrahepatic sulfation of honokiol. SULT1A1 levels are very high in the liver and is also present at lower levels in many other tissues,²⁶ whereas lower mRNA levels have been found for SULT1A2 than for other SULT1A members in the liver, kidney, brain, ovary, and some other sections of the gastrointestinal tract. As recently published data also show the expression of SULT1A2 protein in Caco-2 cells as well as in individual samples of the liver and caecum,^{27,28} our study is indicative of the physiological role of SULT1A2 in honokiol biotransformation. SULT1A3 expression is extremely high in the gut, detectable in many other extrahepatic tissues, and essentially not expressed in the liver,²⁶ whereas SULT1E1 mRNA and protein have been detected in liver, small intestine, and in hormone-dependent tissues (e.g., endometrium and breast). SULT1B1 mRNA has been primarily identified in the liver, small intestine, colon, and blood leucocytes.²⁹ Teubner et al.²⁷ reported a 17-fold higher expression of SULT1B1 in the ileum than in the liver. During absorption, honokiol may be sulfated by several intestinal SULT enzymes, which may contribute to the biotransformation of honokiol.

As observed for glucuronidation, kinetic profiles of M3 formation by four out of six investigated SULT isoforms also exhibited substrate inhibition, but with distinct lower IC_{50} -values of 25–262 μM . The observed decrease in metabolite formation, especially that of the sulfate conjugate at higher honokiol concentrations, may have a major impact on the oral bioavailability of honokiol *in vivo* as saturation and inhibition of M3 formation will not only occur in the intestine but also in the liver. Concomitant oral administration of SULT inhibitors like quercetin or resveratrol with honokiol may substantially increase its bioavailability.

It is not known yet whether honokiol conjugates also exhibit pharmacological activity. However, like the biologically inactive estrogen sulfate and glucuronide that is transformed by cellular sulfatases or by β -glucuronidase into the biological bioactive estradiol,³⁰ honokiol conjugates may also serve as inactive pools for honokiol. Furthermore, conjugation might also prevent honokiol from enzymatic oxidation, extending its half-life in the cell and maintaining its biological properties.³¹

CONCLUSION

Our data demonstrated that honokiol is extensively metabolized in rat and human liver. Glucuronidation and sulfation will therefore play a key role in the elimination of dietary honokiol in humans after oral uptake. Measurements of both parent compound and metabolites will be necessary to correlate pharmacokinetic with pharmacological activity.

ACKNOWLEDGMENTS

This study was supported by grants of the Jubiläumsfonds der Österreichischen Nationalbank (12600) and Fonds zur wissenschaftlichen Forschung (FWF) (P21083-B11) to W. Jäger.

REFERENCES

- Liou KT, Shen YC, Chen CF, Tsao CM, Tsai SK. 2003. The anti-inflammatory effect of honokiol on neutrophils: Mechanisms in the inhibition of reactive oxygen species production. *Eur J Pharmacol* 475:19–27.
- Schühly W, Khan SI, Fischer NH. 2009. Neolignans from North American *Magnolia* species with cyclooxygenase-2 inhibitory activity. *Inflammopharmacology* 17:106–110.
- Shen CC, Ni CL, Shen YC, Huang YL, Kuo CH, Wu TS, Chen CC. 2009. Phenolic constituents from the stem bark of *Magnolia officinalis*. *J Nat Prod* 72:168–171.
- Teng CM, Chen CC, Ko FN, Lee LG, Huang TF, Chen YP, Hsu HY. 1988. Two antiplatelet agents from *Magnolia officinalis*. *Thromb Res* 50:757–765.
- Tsai SK, Huang CH, Huang SS, Hung LM, Hong CY. 1999. Antiarrhythmic effect of magnolol and honokiol during acute phase of coronary occlusion in anesthetized rats: Influence of L-NAME and aspirin. *Pharmacology* 59:227–233.
- Xu Q, Yi LT, Pan Y, Wang X, Li YC, Li JM, Wang CP, Kong LD. 2008. Antidepressant-like effects of the mixture of honokiol and magnolol from the barks of *Magnolia officinalis* in stressed rodents. *Prog Neuropsychopharmacol Biol Psychiatry* 32:715–725.
- Maruyama Y, Kuribara H, Morita M, Yuzurihara M, Weintraub ST. 1998. Identification of magnolol and honokiol as anxiolytic agents in extracts of saiboku-to, an oriental herbal medicine. *J Nat Prod* 61:135–138.
- Kuribara H, Kishi E, Hattori N, Okada M, Maruyama Y. 2000. The anxiolytic effect of two oriental herbal drugs in Japan attributed to honokiol from *Magnolia* bark. *J Pharm Pharmacol* 52:1425–1429.
- Bai X, Cerimele F, Ushio-Fukai M, Waqas M, Campbell PM, Govindarajan B, Der CJ, Battle T, Frank DA, Ye K, Murad E, Dubiel W, Soff G, Arbiser JL. 2003. Honokiol, a small molecular weight natural product, inhibits angiogenesis *in vitro* and tumor growth *in vivo*. *J Biol Chem* 278:35501–35507.
- Wang T, Chen F, Chen Z, Wu YF, Xu XL, Zheng S, Hu X. 2004. Honokiol induces apoptosis through p53-independent pathway in human colorectal cell line RKO. *World J Gastroenterol* 10:2205–2208.
- Battle TE, Arbiser J, Frank DA. 2005. The natural product honokiol induces caspase-dependent apoptosis in B-cell chronic lymphocytic leukemia (B-CLL) cells. *Blood* 106:690–697.
- Wolf I, O'Kelly J, Wakimoto N, Nguyen A, Amblard F, Karlan BY, Arbiser JL, Koeffler HP. 2007. Honokiol, a natural biphenyl, inhibits *in vitro* and *in vivo* growth of breast

- cancer through induction of apoptosis and cell cycle arrest. *Int J Oncol* 30:1529–1537.
13. Hattori M, Sakamoto T, Endo Y, Kakiuchi N, Kobashi K, Mizuno T, Namba T. 1984. Metabolism of magnolol from magnoliae cortex. I. Application of liquid chromatography-mass spectrometry to the analysis of metabolites of magnolol in rats. *Chem Pharm Bull* 32:5010–5017.
 14. Hattori M, Endo Y, Takebe S, Kobashi K, Fukasaku N, Namba T. 1986. Metabolism of magnolol from Magnoliae cortex. II. Absorption, metabolism and excretion of [ring-14C]magnolol in rats. *Chem Pharm Bull* 34:158–167.
 15. El-Ferally FS, Li WS. 1978. Phenolic constituents of *Magnolia grandiflora* L. seeds. *Lloydia* 41:442–449.
 16. Thalhammer T, Stapf V, Gajdzik L, Graf J. 1994. Bile canalicular cationic dye secretion as a model for P-glycoprotein mediated transport. *Eur J Pharmacol* 270:213–220.
 17. Soars MG, Ring BJ, Wrighton SA. 2003. The effect of incubation conditions on the enzyme kinetics of udp-glucuronosyltransferases. *Drug Metab Dispos* 31:762–767.
 18. Fujita M, Itokawa H, Sashida Y. 1973. Studies on the components of *Magnolia obovata* Thunb. 3. Occurrence of magnolol and honokiol in *M. obovata* and other allied plants. *Yakugaku Zasshi* 93:429–434.
 19. Wu X, Chen X, Hu Z. 2003. High-performance liquid chromatographic method for simultaneous determination of honokiol and magnolol in rat plasma. *Talanta* 59:115–121.
 20. Tsai TH, Chou CJ, Cheng FC, Chen CF. 1994. Pharmacokinetics of honokiol after intravenous administration in rats assessed using high-performance liquid chromatography. *J Chromatogr Biomed Appl* 655:41–45.
 21. Tsai TH, Chou CJ, Chen CF. 1996. Pharmacokinetics and brain distribution of magnolol in the rat after intravenous bolus injection. *J Pharm Pharmacol* 48:57–59.
 22. Maier-Salamon A, Hagenauer B, Wirth M, Gabor F, Szekeres T, Jäger W. 2006. Increased transport of resveratrol across monolayers of the human intestinal Caco-2 cells is mediated by inhibition and saturation of metabolites. *Pharm Res* 23:2107–2115.
 23. Miksits M, Maier-Salamon A, Aust S, Thalhammer T, Reznicek G, Kunert O, Haslinger E, Szekeres T, Jaeger W. 2005. Sulfation of resveratrol in human liver: Evidence of a major role for the sulfotransferases SULT1A1 and SULT1E1. *Xenobiotica* 35:1101–1119.
 24. King CD, Rios GR, Green MD, Tephly TR. 2000. UDP-glucuronosyltransferases. *Curr Drug Metab* 1:143–161.
 25. Nagar S, Rimmel RP. 2006. Uridine diphosphoglucuronosyltransferase pharmacogenetics and cancer. *Oncogene* 25:1659–1672.
 26. Glatt, H. 2000. Sulfotransferases in the bioactivation of xenobiotics. *Chem Biol Interact* 129:141–170.
 27. Teubner W, Meinel W, Florian S, Kretzschmar M, Glatt H. 2007. Identification and localization of soluble sulfotransferases in the human gastrointestinal tract. *Biochem J* 404:207–215.
 28. Meinel W, Ebert B, Glatt H, Lampen A. 2008. Sulfotransferase forms expressed in human intestinal Caco-2 and TC7 cells at varying stages of differentiation and role in benzo[a]pyrene metabolism. *Drug Metab Dispos* 36:276–283.
 29. Wang J, Falany JL, Falany CN. 1998. Expression and characterization of a novel thyroid hormone-sulfating form of cytosolic sulfotransferase from human liver. *Mol Pharmacol* 53:274–282.
 30. Otake Y, Nolan AL, Walle UK, Walle T. 2000. Quercetin and resveratrol potentially reduce estrogen sulfotransferase activity in normal human mammary epithelial cells. *J Steroid Biochem Mol Biol* 73:265–270.
 31. Pasqualini JR, Chetrite GS. 2005. Recent insight on the control of enzymes involved in estrogen formation and transformation in human breast cancer. *J Steroid Biochem Mol Biol* 93:221–236.